ELSEVIER

# Site-selective XAFS spectroscopy tuned to surface active sites of copper catalysts

Yasuo Izumi*, Fumitaka Kiyotaki, Hiroyasu Nagamori, Taketoshi Minato

*Department of Environmental Chemistry and Engineering, Interdisciplinary Graduate School of Science and Engineering, Tokyo Institute of Technology, 4259 Nagatsuta, Midori-ku, Yokohama 226-8502, Japan*

## Abstract

To overcome the problem of X-ray absorption fine structure (XAFS) spectroscopy in which the obtained information is the average for all sites in sample, Rowland-type fluorescence spectrometer was designed to measure site-selective XAFS spectra by utilizing the chemical shift of emission peak for each site. Johansson-type cylindrically-bent Ge(111) crystal and scintillation counter were mounted on the spectrometer. The improvement of energy resolution of spectrometer was discussed when the primary beam size and two slit size in the Rowland circle were varied. The energy resolution was ~1.1 eV, smaller than the core-hole lifetime width for Cu $K\alpha_1$ (2.11 eV). The site selection of the $Cu^0$ and $Cu^I$ site-tune spectra was experimentally measured for the physical mixture of Cu metal+CuI and for Cu/ZnO catalyst. Obtained experimental site selection was compared to the theoretical estimations. © 2001 Elsevier Science B.V. All rights reserved.

## 1. Introduction

When X-ray absorption fine structure (XAFS) spectroscopy is applied to the sample which consists of more than one kind of site, obtained information [i.e. bond distances and coordination numbers by extended X-ray absorption fine structure (EXAFS) and normalized X-ray absorption near-edge structure (XANES)] is the average for all sites in sample. Heterogeneous catalysts are typical examples that consist of several kinds of sites. Unique determination of local geometric and electronic structures is

impossible based on conventional XAFS spectroscopy due to this problem.

In this paper, an experimental approach to discriminate each site among co-existing sites in sample is described by utilizing fluorescence spectrometer. A Rowland-type fluorescence spectrometer was settled to analyze fluorescence X-rays from samples in the XAFS measurements. XAFS spectra will be site-selective when the fluorescence spectrometer is tuned to fluorescence peak energy of each site based on the chemical shift of fluorescence X-rays. Dysprosium $L_3$-edge XANES spectrum was reported for dysprosium nitrate by using fluorescence spectrometer [1]. The absorption edge structure was more resolved in the spectrum compared to conventional XANES spectrum. The reason was discussed that the

---

*Corresponding author. Fax: +81-45-924-5569.
*E-mail address:* yizumi@chemenv.titech.ac.jp (Y. Izumi).

XANES spectrum obtained by using fluorescence spectrometer was not affected by the core-hole lifetime broadening because a narrow energy band of the fluorescence radiation was monitored with the fluorescence spectrometer (energy resolution ~0.3 eV) combined with incident beam of high energy-resolution (~0.7 eV) at Wiggler beamline.

Herein, the merits of experimental setup with fluorescence spectrometer are discussed for XANES measurements and the site selection is evaluated for a model sample of both $Cu^0$ and $Cu^I$ sites [physical mixture of copper metal and copper(I) iodide] and Cu/ZnO catalyst in in situ condition. Cu/ZnO is heterogeneous catalyst for methanol synthesis, however, exact active site structure is still open for question because the $Cu^0$ and $Cu^I$ sites co-exist on Cu/ZnO catalysts in in situ conditions.

## 2. Experimental

### 2.1. Design of fluorescence spectrometer

The configuration of high energy-resolution fluorescence spectrometer was illustrated in Fig. 1b in comparison with conventional setup (Fig. 1a). Detailed specification was described in Ref. [2], and improved points for higher energy resolution measurements are summarized. Sample was placed on a plane tilted from horizontal plane, and the Rowland circle of fluorescence spectrometer was in the vertical plane. Top surface of the sample was tilted to the direction of incident X-ray from the horizontal plane (angle $\theta$, Fig. 1b) and also to the direction of the sample (angle $\chi$, Fig. 1b). The angles $\theta$ and $\chi$ were 6–13° during emission and XAFS spectra measurements.

The positions of cylindrically-bent Johansson-type Ge(111) crystal 50(H)×25(V) mm$^2$, $R=220(\pm1)$ mm] and a slit (slit 2, Fig. 1) in front of the NaI(Tl) scintillation counter (SC) were controlled by PC to be precisely on the Rowland circle during emission spectrum scan. Independent control of crystal and detector enables free choice of Rowland radii in the range 127.7–240.9 mm and Bragg angles in the range 83.9–55.6°. This configuration effectively focuses the divergence originally due to the incident
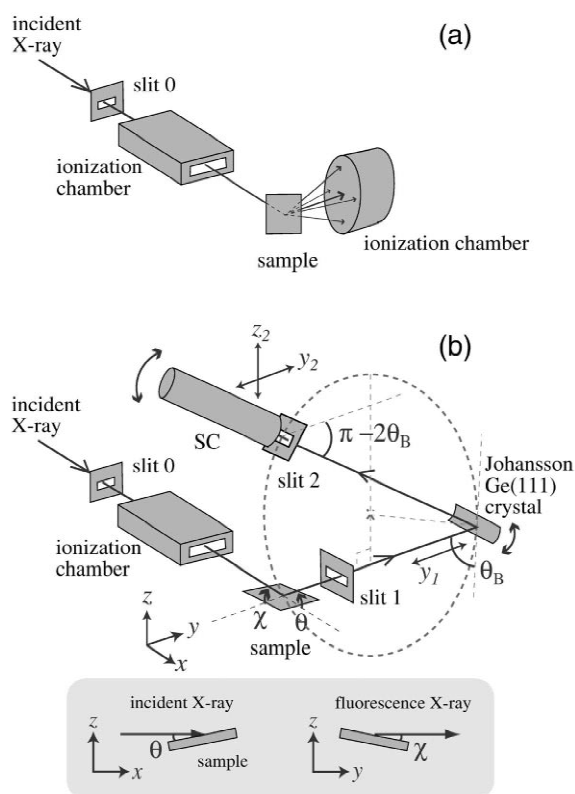


Fig. 1. Configurations of conventional XAFS (a), and of site-selective XAFS by utilizing the fluorescence spectrometer (b).

synchrotron beam (polarized horizontally), and the signal/(back ground) ratio is higher compared to the case of 45°-beam entrance and 45°-beam exit. To realize better energy resolution, the horizontal length of slit 0 and the vertical lengths of slits 1 and 2 are important. These values were optimized within the limit to obtain minimal photon counts at SC for the XANES measurements.

### 2.2. Samples

Copper powder, CuCl, CuCl$_2$, CuBr, CuI, Cu$_2$O, and CuO were used as the standard compounds for emission and/or XANES spectra measurements. Physical mixture of copper metal and CuI was also prepared diluted in boron nitride (BN) matrix (mixed by 1:1 on the basis of Cu amount). Cu/ZnO catalysts

were prepared by the co-precipitation method from Cu and Zn nitrates [3]. The Cu content was 5% (w/w) for all the samples. Obtained powder was calcined at 623 K, followed by heating in hydrogen (53 kPa) at 523 K and in CO (27 kPa)+$H_2$ (27 kPa) at 523 K. The sample was transferred in glass work to an in situ Pyrex cell equipped with a 50-$\mu$m Kapton film on both sides, and sealed by fire. The sample was at room temperature during spectrum measurements.

## 2.3. Emission and XANES spectrum measurements

The Cu K$\alpha$ emission and the Cu K-edge XANES spectra were measured at the Undulator beamline 10XU of SPring-8. The storage ring energy was 8.0 GeV and the ring current was 99–72 mA. Si(111) double crystal monochromator was used. Cu K$\alpha$ emission was monitored with Ge(444) ($d$=0.81652 Å) reflection. The excitation energy was 9000.0($\pm$0.1) eV. The spectrum scan step was 0.0025–0.0100° for the rotation of cylindrically-bent crystal, corresponding to Bragg angle step of 0.12–0.5 eV. The accumulation time of a step was 60–120s. The spectrum energy was calibrated by equalizing the Cu metal K$\alpha_1$ peak to 8047.8 eV [4]. The peak energy positions were reproduced within 0.3 eV when several spectra were scanned at Cu K$\alpha$ by changing the angles $\theta$ and $\chi$ and three slit lengths. The reproducibility was carefully checked especially in the case of smaller length of slits (<0.5 mm) where the photon counts at SC were limited. In the case, both the emission peak shape and the alignment of Rowland-type spectrometer on a level of ~100 $\mu$m were verified.

The $I_0$ beam was monitored by ion chamber filled with nitrogen gas. Site-selective Cu K-edge XANES spectra were measured by tuning the fluorescence spectrometer at 8046.6 and 8049.1 eV for the physical mixture of Cu metal and CuI and at 8046.6 and 8050.9 eV for Cu/ZnO catalyst. The accumulation time of a step was 10–180s. The spectrum energy was calibrated by equalizing the first inflection point of the Cu metal K-edge to 8980.3 eV [4].

Site selection for the site-selective XANES was evaluated by the fitting with the convolution of

conventional XANES spectra. The ratio of conventional XANES spectra was varied between 10:0 and 0:10, and the fit was evaluated based on the $R$ factor $(R_\mathrm{f}) = \int |\chi(\mathrm{exp}) - \chi(\mathrm{fit})|^2 \, dE / \int |\chi(\mathrm{exp})|^2 \, dE$.

## 3. Results

### 3.1. Line widths and chemical shifts of the emission spectra

Cu K$\alpha$ emission spectra were measured for Cu metal, CuCl, $CuCl_2$, the physical mixture of Cu metal and CuI, and the Cu/ZnO catalyst. The peak top and FWHM (full width at a half maximum) were evaluated based on the fitting with a Gaussian and/or a Lorentzian function(s) and flat background. The peak top energy shifted by +1.6 eV on going from Cu metal to CuCl and by −0.6 eV on going from CuCl to $CuCl_2$. The FWHM values varied according to the changes of horizontal length of slit 0 and vertical lengths of slits 1 and 2 (Fig. 1b). The FWHM for Cu K$\alpha_1$ peak was as small as 2.4 eV (Fig. 2c) when the sizes of slits 0–2 were 2.0(H)× 1.0(V), 8.0(H)×0.5(V), and 8.0(H)×0.5(V) $mm^2$, respectively. Note that the improvement of monochromator, i.e. smaller beam size at sample, was also important for better energy resolution of fluorescence spectra. The FWHM value was 3.0 eV with the same three slits sizes during the beamtime of 1999, when old Si(111) crystals were used for monochromator. New Si(111) crystals with better crystallinity were used for monochromator during the beamtime of 2000, and smaller FWHM of 2.4 eV was enabled.

The Cu K$\alpha$ peaks for Cu/ZnO heated in CO+$H_2$ at 523 K shifted by 0.6–0.9 eV compared to the Cu metal (Fig. 2a,b). The shift may correspond to $Cu^{II}$ site [5], however, wider peak width (4.0 eV for Cu/ZnO vs. 3.5 eV for Cu metal) suggested that the Cu/ZnO catalyst consisted of $Cu^0$ and $Cu^I$ sites and the emission spectra were the convolution of the two contributions. The peak energy position for the physical mixture of Cu metal and CuI was also between those of Cu metal (Fig. 2c) and CuI, and the peak width for the physical mixture of Cu metal and CuI was wider than that of Cu metal or CuI.
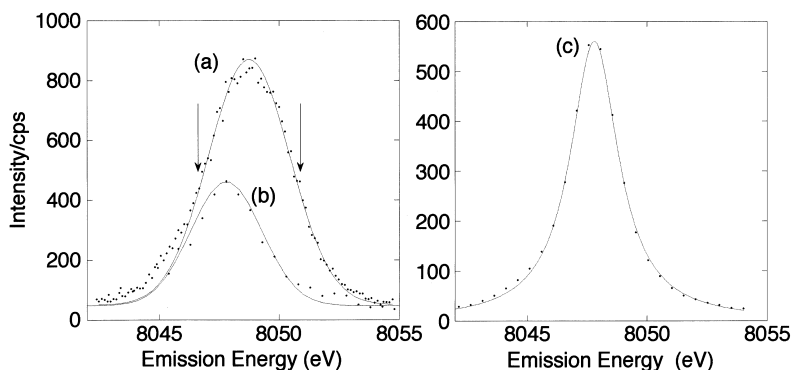
Fig. 2. Cu K$\alpha_1$ emission spectra for Cu/ZnO catalyst (a) and Cu metal (b). The energy resolution was improved at the beamtime of 2000 for Cu metal (c). The experimental data are plotted as points and the Gaussian/Lorentzian fittings are drawn as solid lines. Two arrows indicate tune energies for site-selective XAFS measurements.

### 3.2. Site-selective XANES spectra for the physical mixture of Cu metal and CuI

The fluorescence spectrometer was tuned to 8046.6 eV (tuned to $Cu^0$ site) and 8049.1 eV (tuned to $Cu^I$ site) for the physical mixture of Cu metal and CuI based on the Cu K$\alpha_1$ emission spectra. Obtained XANES spectra were shown in Fig. 3a and b, respectively. The latter pattern was essentially the same as that for CuI (Fig. 3e) whereas the former pattern was not the same as that for Cu metal. The $R_f$ value (see its definition in Section 2) reached the minimum at the ratio of Cu metal (Fig. 3d):CuI spectra (Fig. 3e) = 60($\pm$10):40($\pm$10) (minimum $R_f$ = 1.6%) for Fig. 3a and at the ratio of Cu metal:CuI

spectra = 10($\pm$10):90($\pm$10)   (minimum $R_f$ = 0.3%) for Fig. 3b.

### 3.3. Site-selective XANES spectra for the Cu/ZnO catalyst

The conventional fluorescence XANES spectrum for the Cu/ZnO catalyst (Fig. 4c) did not have a shoulder at 8988 eV nor a peak at 9000 eV, which were typical for XANES for CuO (Fig. 4h). The possibility that the $Cu^{II}$ site co-exists in the Cu/ZnO catalyst in in situ condition can be neglected, and the targets of site-selective XANES became $Cu^0$ and $Cu^I$ sites. The fluorescence spectrometer was tuned to
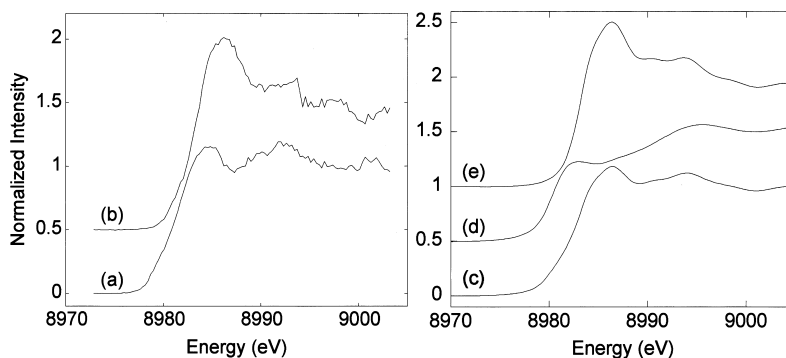


Fig. 3. Site-selective XANES spectra for the physical mixture of copper metal and copper(I) iodide. The fluorescence spectrometer was tuned to 8046.6 eV (a) and 8049.1 eV (b). Conventional fluorescence XANES spectra for the physical mixture of Cu metal + CuI (c), Cu metal (d), and CuI (e). All the samples were diluted in boron nitride matrix to Cu 5% (w/w).
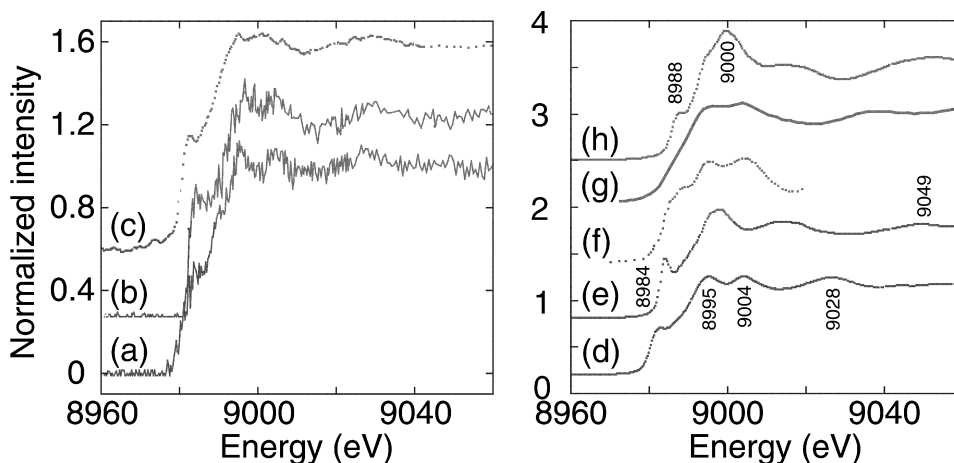
Fig. 4. Site-selective XANES spectra for Cu/ZnO catalyst. Fluorescence spectrometer was tuned to 8046.6 eV (a) and to 8050.9 eV (b). Conventional XANES spectra for Cu/ZnO (c), Cu metal (d), $Cu_2O$ (e), $[Cu\{N(CH_2CH_2\text{-}2\text{-pyridyl})_3\}][BPh_4]$ (f), and CuO (h) were measured by Lytle detector (c) or in transmission mode (d,e,h). XANES was theoretically generated by FEFF8 for $Cu^I$ atomically dispersed on ZnO (g). Spectrum (f) was reproduced from Ref. [6].

8046.6 and 8050.9 eV, respectively, based on the emission spectrum (Fig. 2, arrows).

The site-selective XANES tuned to 8046.6 eV (Fig. 4a) resembled XANES for Cu metal (Fig. 4d). The rising-edge energy position shifted to higher energy for site-selective XANES tuned to 8050.9 eV (Fig. 4b), demonstrating the contribution from the $Cu^I$ site. The peak top position at 8984 eV was the same as that of XANES for $Cu_2O$ (Fig. 4e). The region of 8993–9008 eV was intense, similar to the case of $Cu_2O$, though the peak split into two peaks. The peak position 9028 eV was the same as that of Fig. 4d for Cu metal.

Obtained site-selective spectra were fit by standard spectra in Fig. 4d–h. The XANES spectrum for $Cu^I$ site atomically dispersed on wurzite ZnO(0001) surface (Fig. 4g) was generated by FEFF8 for a model cluster within 6 Å from the Cu center in a self-consistent field and multiple scattering modes [7,8]. The theoretical XANES was similar to XANES of model complex $[Cu\{N(CH_2CH_2\text{-}2\text{-pyridyl})_3\}][BPh_4]$ (Fig. 4f). Based on the criteria that the $R_f$ values reached the minimum, $Cu^0$ and $Cu^I$ site-selective XANES were best fit with $80(\pm10):20(\pm10)$ mixture of XANES for Cu metal + $Cu_2O$ and $50(\pm10):25(\pm10):25(\pm10)$ mixture of XANES for Cu metal + $Cu_2O$ + $Cu^I$ atomical-

ly dispersed on ZnO surface, respectively. As the conventional XANES for Cu/ZnO catalyst (Fig. 4c) was best fit with $70(\pm10):30(\pm10)$ mixture of $Cu^0$ and $Cu^I$ site-selective XANES [3], the Cu site ratio was estimated to be Cu metal:$Cu_2O$:$Cu^I$ atomically dispersed on ZnO surface = $70(\pm23):22(\pm14):8(\pm5)$ for Cu/ZnO catalyst in in situ condition.

## 4. Discussion

### 4.1. Estimation of energy resolution

The energy resolution of wave number-dispersive spectrometer was formulated as:

$$\Delta E/E = \cot\theta_B\,\Delta\Theta \qquad (1)$$

The $\Delta\Theta$ was formulated for bent crystal as the effects of geometrical angle width, the divergence of beam perpendicular to the Rowland circle plane, and the X-ray penetration depth into the crystal [9]:

$$\Delta\Theta =$$
$$\frac{[(W_s + W_f)^2 + (h^2/8R\cos\theta_B)^2 + \{(2\cos\theta_B\sin\theta_B\ln2)/\mu\}^2]^{1/2}}{8R\sin\theta_B}$$

$$(2)$$

where $W_s$ is the effective source size in the plane of diffraction, $W_f$ is the slit width (vertical in Fig. 1b) on Rowland circle in front of SC, $\mu$ is the absorption coefficient of crystal, $h$ is the slit length (horizontal in Fig. 1b), and $R$ is the Rowland radius. Thus:

$$\Delta E = E \cot \theta_B \, \Delta\Theta$$

$$\sim \frac{E^3(2d)^2}{8RC^2}\left[(W_s + W_f)^2 + \left(\frac{h^2}{8R}\right)^2 + \left(\frac{CE^2 \ln 2}{Kd}\right)^2\right]^{1/2} \quad (3)$$

where $E$ is the fluorescence X-ray energy, $d$ is the lattice constant of crystal, and $C$ is a constant (12.398 keV Å). $K$ is the approximation of $\mu E^3$. The $\Delta E$ was evaluated to be 2.5 eV based on the angle $\chi$ ($= 7°$) at $E = 8.05$ keV and $d_{Ge(444)} = 0.81652$ Å. This value was in accord with the experiments on 1999 [2]. The FWHM value during the experiments on 2000 was 2.4 eV. Assuming the Gaussian shape peak convolution of the width due to experimental apparatus and core-hole lifetime width, improved energy resolution of the spectrometer was estimated to be 1.1 eV. This value includes the energy resolution of primary beam of beamline [1]. This resolution corresponds to $W_s = W_f = 0.11$ mm in Eq. (3). As the beam height was approximated to be slit length(H)×tan $\chi$, the effective primary beam width(H) was calculated to ~0.90 mm. Hence, the beam size decrease owing to the improvement of

monochromator of beamline 10XU should be the major reason for the better energy resolution in the case of measurements on 2000.

## 4.2. Estimation of site selection based on the energy resolution

The site selection by detecting Cu K$\alpha_1$ peak in the case of energy resolution of spectrometer $= 1.1$ eV is estimated, and compared to the site-selective experiments for the physical mixture of Cu metal and CuI (Fig. 3). The chemical shift on going from Cu$^0$ to Cu$^I$ was relatively large ($+1.6$ eV) for Cu metal and CuCl, however, the shifts were relatively smaller for CuBr, CuI, or Cu$_2$O (0.1–0.8 eV) compared from Cu metal [10]. Therefore, two examples of chemical shifts of 1.6 and 0.8 eV were plotted in Fig. 5a and b, respectively. The two dotted peaks have the FWHM of core-hole lifetime width (Cu K+L$_3$ 2.11 eV [11]) were separated by chemical shift of 1.6 eV (a) and 0.8 eV (b). The two solid peaks with the FWHM of estimated energy resolution of spectrometer (1.1 eV) were separated by 2.47 eV, tune energy gap in the site-selective measurements of Fig. 3 (8046.6 and 8049.1 eV in the cases of Cu$^0$ and Cu$^I$ site-tune, respectively). The ratio of overlap area (hatched) estimates site selection. The site selection was 82% (a) and 69% (b). The site selection as a function with chemical shift was plotted in (c).

The unequal site selection, i.e. 60 vs. 90% of Cu$^0$
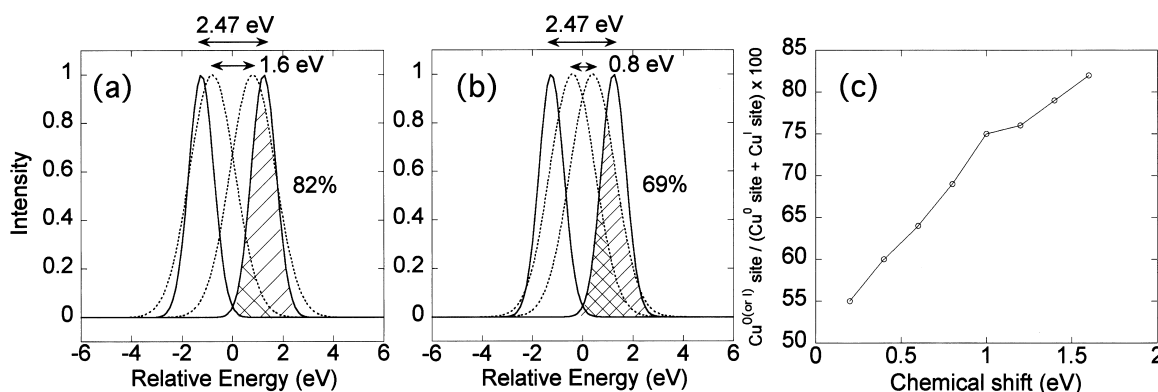


Fig. 5. The estimation of site selection for Cu K$\alpha_1$. The two dotted peaks with the FWHM of core-hole lifetime width (2.11 eV) were separated by chemical shift of 1.6 eV (a) and 0.8 eV (b). The two solid peaks with the FWHM of estimated energy resolution of spectrometer (1.1 eV) were separated by 2.47 eV. The ratio of overlap area (hatched) estimates site selection. The site selection as a function with chemical shift is plotted in (c).

and $Cu^I$ site tunes, cannot be explained only based on peak overlap in Fig. 5. One of the possibilities is the energy shift due to the unsymmetric nature of emission peak or the problem of Bragg angle reproducibility (e.g. stepping motor backlash, etc.). If the two tune energies ($+1.235$ and $-1.235$ eV, solid peaks in Fig. 5b) shifted by $+0.8$ eV, i.e. $+2.035$ and $-0.435$ eV), the site selection is estimated to be 56 ($Cu^0$ site tune) and 77 ($Cu^I$ site tune). These values support experimental trends in site-selective XANES measurements: $60(\pm10)\%$ for $Cu^0$ site tune (Fig. 3a) and $90(\pm10)\%$ for $Cu^I$ site tune (Fig. 3b).

## 5. Conclusions

The site-selective XANES measurements were performed for a model system of copper catalyst (physical mixture of Cu metal and CuI diluted in BN) by utilizing a fluorescence spectrometer. The energy resolution of fluorescence spectrometer was as small as 1.1 eV, including the energy resolution of beamline monochromator, at the Cu $K\alpha_1$ emission energy, smaller than core-hole lifetime width (2.11 eV). The site selection was estimated to be $60(\pm10)$ and $90(\pm10)\%$ for $Cu^0$ and $Cu^I$ site-tune spectra, respectively. Theoretical estimation was $\sim56$ and $\sim77\%$ based on the overlap of two peaks with the width of core-hole lifetime and a peak with the width of energy resolution of spectrometer. This method was also applied to Cu/ZnO catalyst in in situ condition. The population of sites was estimated to be Cu metal:$Cu_2O$:$Cu^I$ atomically dispersed on ZnO surface$=70(\pm23):22(\pm14):8(\pm5)$.

## References

[1] V. Stojanoff, K. Hamalainen, D.P. Siddons, J.B. Hastings, L.E. Berman, S. Cramer, G. Smith, Rev. Sci. Instrum. 63 (1992) 1125–1127.

[2] Y. Izumi, H. Oyanagi, H. Nagamori, Bull. Chem. Soc. Jpn. 73 (2000) 2017–2023.

[3] Y. Izumi, H. Nagamori, Bull. Chem. Soc. Jpn. 73 (2000) 1581–1587.

[4] J.A. Bearden, Rev. Mod. Phys. 39 (1967) 78–124.

[5] B.S. Clausen, B. Lengeler, B.S. Rasmussen, J. Phys. Chem. 89 (1985) 2319–2324.

[6] L. Kau, K.O. Hodgson, E.I. Solomon, J. Am. Chem. Soc. 111 (1989) 7103–7109.

[7] A.L. Ankudinov, B. Ravel, J.J. Rehr, S.D. Condradson, Phys. Rev. B 58 (1998) 7565–7576.

[8] J.J. Rehr, J. Mustre de Leon, S.I. Zabinsky, R.C. Albers, J. Am. Chem. Soc. 113 (1991) 5135–5140.

[9] P. Georgopoulos, G.S. Knapp, J. Appl. Crystallogr. 14 (1981) 3–7.

[10] F. Kiyotaki, T. Minato, Y. Izumi, in preparation.

[11] M.O. Krause, J.H. Olivier, J. Phys. Chem. Ref. Data 8 (1979) 329–338.